FRET Probes as a Technique for Determining the Catalytic Activity of Enzymes in the Model Biomembranes Systems and Further in the Living Cells

Igor Dmitrievich Zlotnikov , Alexander A. Ezhov , Elena V. Kudryashova *

Posted Date: 31 May 2024

doi: 10.20944/preprints202405.2096.v1

Keywords: FRET probes; marker; rhodamine 6G; reverse micelle; intracellular enzyme activity

 doi:10.20944/preprints202405.2096.v1

Article

Intermolecular FRET Pairs as an Approach to Visualize Specific Enzyme Activity in Model Biomembranes and Living Cells

Igor D. Zlotnikov [1], Alexander A. Ezhov [2] and Elena V. Kudryashova[1,*]

[1] Faculty of Chemistry, Lomonosov Moscow State University, Leninskie Gory, 1/3, 119991 Moscow, Russia; zlotnikovid@my.msu.ru (I.D.Z.);
[2] Faculty of Physics, Lomonosov Moscow State University, Leninskie Gory, 1/2, 119991 Moscow, Russia;
* Correspondence: helenakoudriachova@yandex.ru

Abstract: Here we proposed an analytical approach based on the intermolecular fluorescent resonant energy transfer (FRET) pairs to visualization of the specific enzyme activity in model biomembranes and in the living cells. The enzyme catalyzes the reaction with the release of a fluorescent product, the signal from which may be quenched or insufficiently selective to allow life-sciences applications. With the FRET technique, we can enhance the selectivity of fluorescent detection of enzyme activity by shifting the maximum emission wavelength to the longer-wavelength range and reduction the influence of medium components. As fluorescence donors, we have used derivatives of 4-methylumbelliferone (MUmb) and 7-amino-4-methylcoumarin (AMC), which also serve as substrates for hydrolases such as chymotrypsin, phosphatase, and asparaginase. During the catalytic depletion of substrates, an accumulation of a highly fluorescent product is observed. This product can be specifically detected using the fluorescent marker rhodamine 6G (R6G), which emits light in the red region of the spectrum (550–600 nm) with high quantum yield. A significant FRET effect is observed when forming AOT reverse micelles. This is due to the proximity of fluorophores within the hydrophobic core of the micelle, which is shorter than in a buffer solution. This allows to monitor the enzymatic reaction selectively (by R6G emission in the red region, 550-600 nm), and obtain a significantly higher fluorescence yield (by an order of the magnitude). This approach has further implications for visualizing intracellular processes. The FRET technique can be used to determine intracellular enzymatic activity by detection with confocal laser scanning microcopy (CLSM), as demonstrated with L-asparaginase, a clinically important anti-leukemia medication. The approach suggested will allow to study enzyme activity within cells. This has the potential to revolutionize medicine by improving drug development and shedding light on previously unknown aspects of cellular metabolism. So, we have shown that the method suggested has good potential in visualization of enzyme functioning inside the living cells, which is often a challenging task. Shift of the fluorescence signal to the long-wavelength region would increase the signal selectivity, making it easily distinguishable from autofluorescence.

Keywords: FRET probes; marker; rhodamine 6G; reverse micelle; intracellular enzyme activity

1. Introduction

The paper is devoted to the study of the potential application of the effect of fluorescent resonant energy transfer (FRET [1–14]) as a selective indicator for various biochemical phenomena, in particular the catalytic activity of enzymes in the model biomembrane systems, with an eye on the enzyme activity registration in living cells. Micellar enzymology is an interesting field for the application of FRET [15–17]. Here we use FRET to modify existing methods or to track certain reaction mechanisms. Why it may be necessary to determine enzymatic activity using the FRET technique? Firstly, the shift of the emission maximum to the long-wavelength region and the obtaining of a system with a higher quantum yield, which would open up the possibility of applying an approach to the visualization of processes in cells using confocal laser scanning microcopy (CLSM) [2,18–20].

 doi:10.20944/preprints202405.2096.v1

Secondly, the FRET technique can reduce fluorescence quenching, particularly in model biomembrane systems such as liposomes and reverse micelles. It is possible to choose appropriate fluorophore acceptors depending on the goals and conditions of the experiment.

In the last decade, the use of (FRET) as a technique for measuring biochemical parameters has been actively explored. This tool has proven to be effective due to its sensitivity and specificity. The FRET effect depends on the specific arrangement of molecules in a system, making it a valuable tool for studying biological processes.

Changes in the FRET signal can be monitored in real-time, providing information about the system's state – and immediately note that it would be extremely difficult to visualize, for example, cellular processes in any way other than using FRET. FRET has also been used to create powerful sensors for biological research and medical applications, such as creating sensors for detecting specific molecules or detecting changes in cell behavior [21–24].

The FRET signal increases dramatically when three conditions coincide: 1) overlapping of the emission spectra of the fluorescence of the donor and the absorption of the acceptor, 2) convergence of the fluorophores at a distance of about 2-8 nm, 3) orientation of the dipoles at an angle significantly different from the straight one - these are quite specific conditions. With regard to the catalytic activity of enzymes, a change in the FRET signal should be considered, which occurs for the following reasons: 1) An increase in the emission coefficient of the product compared with the substrate (coumarin and umbelliferon derivatives are often used), 2) a decrease in steric difficulties for the orientation and convergence of donor and acceptor molecules.

In this work, as a fluorophore acceptor we used rhodamine 6G (R6G) based FRET probes [25–29] to study the activity of enzymes of different class (chymotrypsin, asparaginase, phosphatase) in 1) a aqueous buffer solution, 2) reversed micelles system in which fluorophore molecules are close to each other due to the small volume of the aqueous phase in comparison with an aqueous solution, 3) in living cells. Derivatives of methylumbelliferone (MUmb) and coumarin were used as enzyme substrates, which were converted by a catalyst into products following by FRET-marker R6G manifestation.

This approach can be used both to study the catalytic activity of enzymes in micelles, (as relevant model of biomembrane system) and further it can be applied to visualize the enzyme functioning in the living cells in the condition of their localization in specific cellular structures with for example CLSM technique, where fluorescent probes in the visible area are required with high resolution and signal selectivity (to exclude the autofluorescence).

2. Materials and Method

2.1. Reagents

Surfactant AOT (Aerosol OT, sodium bis(2-ethylhexyl) sulfosuccinate); the fluorophores rhodamine 6G (R6G), 4-methylumbelliferyl p-trimethylammoniocinnamate chloride (MUTMAC), 4-methylumbelliferyl phosphate (MUmb-phosphate), 4-methylumbelliferone (MUmb), L-aspartic acid β-(7-amido-4-methylcoumarin) (Asp-AMC), 7-amino-4-methylcoumarin (AMC) were purchased from Sigma-Aldrich (St Louis, USA).

Enzymes: α-chymotripsin from bovine pancreas (EC 3.4.21.1, ≥40 units/mg protein), acid phosphatase (EC 3.1.3.2), alkaline phosphatase (EC 3.1.3.1) – were purchased from Sigma-Aldrich (St. Louis, MI, USA). Recombinant L-asparaginase from *Erwinia carotovora* (EwA) used in this work was isolated following expression in constructed stain *E. coli* BL21(DE3)/pACYC_LANS (KM). The activity of asparaginase was checked using the method of circular dichroism spectroscopy on device J-815 CD spectrometer (Jasco, Tokyo, Japan).

2.2. FRET Probes for Determining the Catalytic Activity of Enzymes

2.2.1. FRET Probes

 doi:10.20944/preprints202405.2096.v1

The FRET pairs consisted of a donor (enzyme substrate and catalytic reaction product) and an acceptor (R6G). The final concentration of fluorophores was 1 μg/mL. Fluorophore emission and excitation spectra were recorded for each separately and for a donor+acceptor mixture in a buffer solution (PBS 0.01M, pH 7.4).

The excitation and emission spectra of fluorescence were recorded on the device Varian Cary Eclipse fluorescence spectrometer (Agilent Technologies, Santa Clara, CA, USA). FRET efficiency E was calculated as $E = 1 - F_{DA}/F_D$. Where F_{DA} and F_D – the intensities of donor fluorescence in the presence and absence of the acceptor, respectively; F_{AD} and F_A – the intensities of acceptor fluorescence in the presence and absence of the donor, respectively. In the other hand, $E = 1/(1 + (R/R_0)^6)$, where R_0 - the Förster radius is the distance at which 50% of the excitation energy is transferred from the donor to the acceptor, it is about 5-6 nm in the studied systems. So, $r = R_0 \times (1 / (F_D/F_{DA} - 1))^{1/6}$.

2.2.2. Fluorometric Determination of Enzyme Activity

The catalytic activity of enzymes was determined fluorometrically: 1) in a buffer solution; 2) in a reversed micellar system; 3) in living cells. The reaction rate was measured by the accumulation of the fluorescent reaction product and R6G FRET agent: specific parameters are indicated in the captions to the tables and figures.

To make a solution of reversed micelles with a given hydration degree (W_0), a certain amount of PBS buffer solution (Vaq) was added to 1 mL of micellar solution (Vmic) based on the formula $Vaq = 18 * C_{AOT} * W_0$ (μL), where C_{AOT} is the concentration of AOT equal to 0.1 M. The resulting mixture was vigorously shaken until a homogeneous optically transparent solution was formed.

To determine the intracellular activity of L-asparaginase, an enzyme sample (0.5 mg/mL) was incubated with HEK293T cells for 1-4 h at 37 °C, then the cells were thoroughly washed of unabsorbed protein. 5% agarose gel containing 1 mg/mL of MUTMAC substrate and 1 μM FRET-agent R6G was prepared. Then, 100 μl of fluorescent gel was added to a suspension of 100 μl of HEK293T cells in a 96-well plate and intensively mixed. The gel solidified for several minutes. The samples were then incubated for 4 hours at 37 °C for the enzymatic reaction to take place. Cells were visualized using a confocal microscope Olympus FluoView FV1000, which was equipped with both a spectral version scan unit with emission detectors and a transmitted light detector. The product was developed by fluorescence of the FRET-agent R6G: λ_{exci} = 515 nm, λ_{emi} = 540-600 nm. The scan area was 80 × 80 μm². Olympus FV10 ASW 1.7 software was used for the acquisition of the images.

2.3. HEK293T Cells Cultivation

The embryonic kidney human epithelium HEK293T cell line was obtained from the Lomonosov Moscow State University Depository of Live Systems Collection (Moscow, Russia). Cells were grown in RPMI-1640 medium (Gibco, Thermo Fisher Scientific Inc., Waltham, MA, USA) supplemented with 5% fetal bovine serum (Capricorn Scientific, Ebsdorfergrund, Germany) and 1% Na-pyruvate (Paneco, Moscow, Russia) at 5% CO2/95% air in a humidified atmosphere at 37 ◦C.

3. Results and Discussion

3.1. FRET Probes Spectral Properties

To study the enzymatic activity, we used MUmb-based fluorescent substrates MUTMAC (substrate for protease, α-chymotrypsin), MUmb-phosphate (substrate of phosphatase), Asp-AMC (substrate of L-asparaginase). The products of these biocatalytic reactions, respectively, MUmb, MUmb and AMC – have 1-2 orders of magnitude higher emission coefficient than substrates (Figure 1). The product served as a fluorescence donor for R6G. In the normalized form (Figure 1), there is obviously a more effective overlap of the fluorescent spectra of the donor and acceptor in the case of products compared to substrates, which further enhances the signal-to-background ratio.

 doi:10.20944/preprints202405.2096.v1

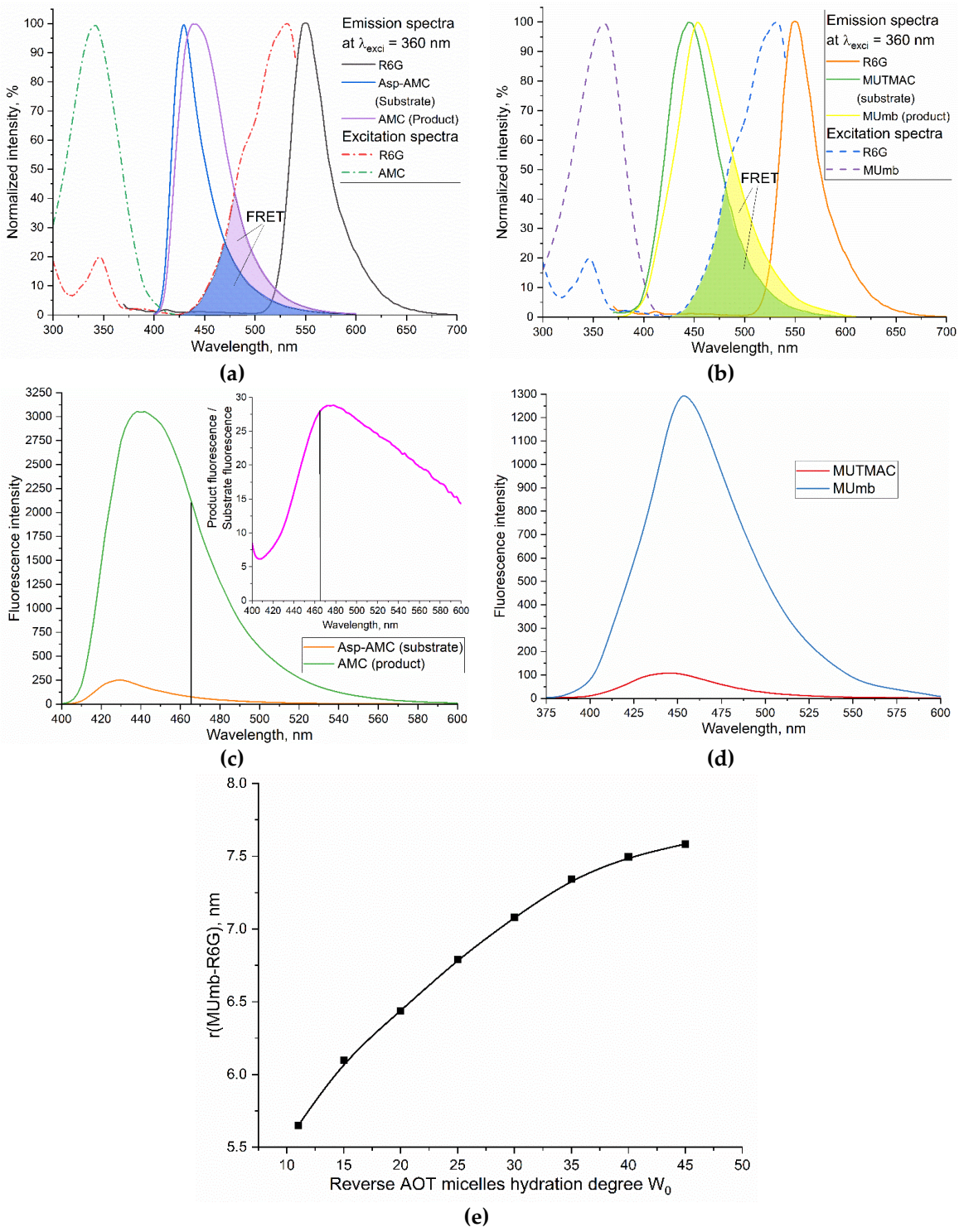

Figure 1. (a) Normalized fluorescence spectra of R6G, Asp-AMC and AMC (1 μM) in PBS buffer solution (0.01M, pH 7.4). **(b)** Normalized fluorescence spectra of R6G, MUTMAC and MUmb (1 μM) in PBS buffer solution (0.01M, pH 7.4). The excitation wavelength is 360 nm. The emission wavelength is 550 nm for R6G and 440-460 nm for AMC and MUmb-derivatives. T = 37 °C. **(c)** Fluorescence emission spectra of Asp-AMC (1 μM) in comparison with AMC (1 μM) in PBS buffer solution (0.01M, pH 7.4), λ_{exci} = 360 nm. **(d)** Fluorescence emission spectra of MUTMAC (0.25 μM) in comparison with MUmb (1 μM) in PBS buffer solution (0.01M, pH 7.4), λ_{exci} = 360 nm. T = 37 °C. **(e)** The distance between the fluorophores of the MUmb-R6G FRET pair, depending on the composition of the AOT/octane micellar system.

 doi:10.20944/preprints202405.2096.v1

3.2. Monitoring the Enzyme Catalytic Activity in Buffer Solution vs Reversed Micellar Systems Using FRET Probes

3.2.1. Theoretical Comparison of Expected FRET Effects in a Buffer and in a System of Reverse Micelles

Previously, we demonstrated that the FRET effect is not as pronounced in aqueous solutions, whereas in micellar systems, this effect is significantly stronger [7]. FRET probes are further applied to study the enzymatic activity in the membrane-like systems such as reverse micelles. While in classical surfactant micelles, enzymes tend to denature, the use of reversed micelles makes it possible to solubilize enzymes while maintaining or even enhancing their catalytic activity [30–33].

Reverse micelles spontaneously form in a tertiary system containing surfactant, water and non-polar organic solvent. The size of the inner cavity of micelles where protein molecules and other hydrophilic molecules can be entrapped can be strictly controlled by varying the surfactant hydration degree (W_0), which represents the molar ratio of water to surfactant. Reverse micelles can be considered as a "nanoreactor" of molecular size where one can obtain the desired supramolecular form of the protein or its complexes by controlling of the micellar inner cavity size. The method therefore provides the modulation of the enzyme activity and oligomeric composition, as it has been demonstrated for a number of enzymes of different classes [30–33].

This approach is perspective to study the membrane enzymes functioning details and to determine the influence of the membrane lipid compositions on the catalytic activity. For example, the reverse AOT micelles are relevant models of mitochondrial membranes. It is known that the mitochondrial membranes contain non-bilayer lipid structures consisting of associates of lipid molecules arranged as reverse micelles incorporated between monolayers of the bilayer membrane. Water–AOT–isooctane is one of the most intensively studied reverse micellar systems for membrane-protein studying [44–48]. Additionally, reversed AOT-octane micelles are often used to study enzymatic activity to investigate catalytic processes in non-aqueous media and to synthesize or analyze hydrophobic substances. However, in such complex systems due to high background level, low fluorophore quantum yield, unsuitable observation wavelength that interferes with other components of the system, special conditions are required to selective product detection, such as high sensitivity and signal selectivity. This can be achieved with FRET approach developing here. With this in mind, we applied FRET approach to study the enzyme activity in reverse micelles.

3.2.2. Objects of Research

Here we consider α-chymotrypsin, acid and alkaline phosphatase and L-asparaginase as model membranotropic as well as membrane independent enzymes catalyzing MUmb or AMC derivatives with the release of MUmb/AMC - fluorophores.

FRET is observed in aqueous solution for between MUmb-derivative and R6G, but the FRET effect is rather weak, since the donor and acceptor molecules separated from each other in the volume of the solution [7]. A different situation is observed for reverse micellar system, where the enzyme and the reaction components are located in a limited volume of the aqueous phase of the inner cavity of the micelles.

The fluorescent substrate based on MUmb derivatives is convenient for a number of enzymes. During their enzymatic hydrolysis, the fluorescent product MUmb is released. This effect can be visualized and amplified by FRET: the enzymatic reaction can be monitored by ascending fluorescence of R6G-marker (acceptor) – at 550 nm wavelength. The product release (MUmb) was used as a control parameter, which is reflected in an increase in fluorescence at 450 nm. In reversed micelles, FRET is expected to be more pronounced, due to concentration of the enzyme and the reaction components in the aqueous phase of the micellar system: MUmb or AMC will be closer to the acceptor R6G, the distance **R** between the fluorophores decreases, the effectivity of the FRET (**E**) is greater: $E = 1/(1 + (R/R_0)^6)$, where R_0 - the Förster radius is the distance at which 50% of the excitation energy is transferred from the donor to the acceptor, it is about 5-6 nm in the studied systems.

 doi:10.20944/preprints202405.2096.v1

3.2.3. FRET Enhancing due to α-Chymotrypsin Activity in AOT-Isooctane Reverse Micelles

The enzymatic activity of α-chymotrypsin in reversed micelles by increase in the fluorescence intensity of R6G-acceptor due to FRET effect was studied in comparison with such a defined by accumulation of the initial product (MUmb – Figure 2a). In AOT-octane reversed micelles, an optimum activity (determined by the enzyme molecule size) for α-chymotrypsin is observed at the hydration degree of W_0 = 11 (Figure 2b), where is the size of the inner cavity of the micelles corresponding to the geometric size of the enzyme monomer [32]. α-Chymotrypsin catalyzes the hydrolysis reaction of MUTMAC to MUmb (Figure 2a) in the reversed micellse. It turned out that the enzymatic activity at a wavelength of 450 nm (assigned to MUmb) characterized by low sensitivity compared to aqueous solution, since the fluorescence of the product is quenched in the micellar system (by more than 45%).

When FRET effect is realized by including of fluorophore acceptor R6G in the reversed micelles, the sensitivity of the signal increases sharply due to an order of magnitude higher molar emission coefficient of R6G compared to MUmb. Figure 2c shows the sensitivity indexes (the rate of the MUTMAC hydrolysis reaction in the presence of FRET-agent R6G / in the absence of R6G) for determining the rate of MUTMAC hydrolysis reaction in the presence of FRET-agent R6G vs in the absence of R6G. In the buffer solution and in the system of reversed micelles, the dependence of the sensitivity index on the R6G concentration has a maximum at the C_{R6G} = 5 and 10 μM, respectively. This is equivalent to MUTMAC:R6G ratios of 40 and 20 (mol/mol), respectively. In the buffer solution, the sensitivity does not exceed 0.25-0.3, which is due to the low efficiency of the FRET. On the contrary, in a system of reversed micelles, it is difficult to monitor the enzymatic reaction by MUTMAC/MUmb at 450 nm due to the quenching of the product signal, therefore, the sensitivity index for the FRET marker is about 2-3 units. The data obtained using the new FRET approach are consistent with the literature [34–36].

When using small micelles with a degree of hydration of 11, the distance between the fluorophores of the FRET pairs approaches the value R_0 ~ 5.5 nm (Figure 1e), which determines the high sensitivity of the FRET method (Figure 2c) in a system of reversed micelles with low degrees of hydration.

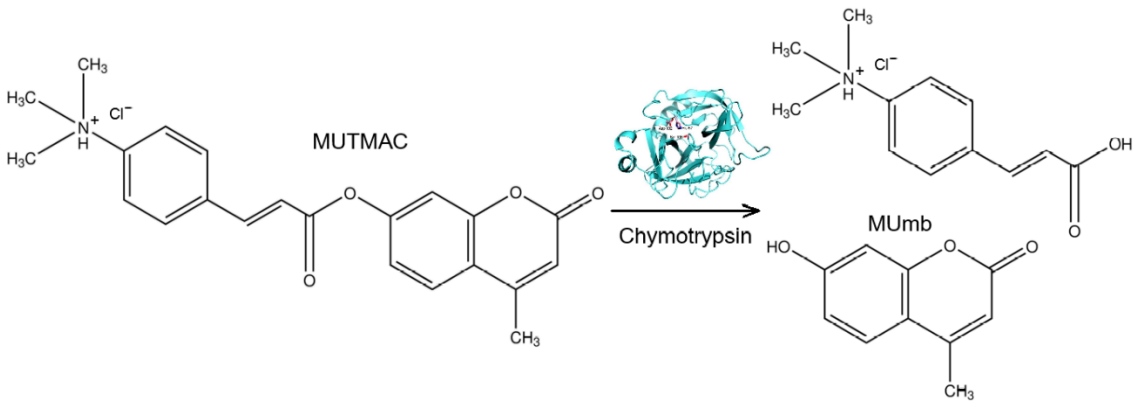

(a)

 doi:10.20944/preprints202405.2096.v1

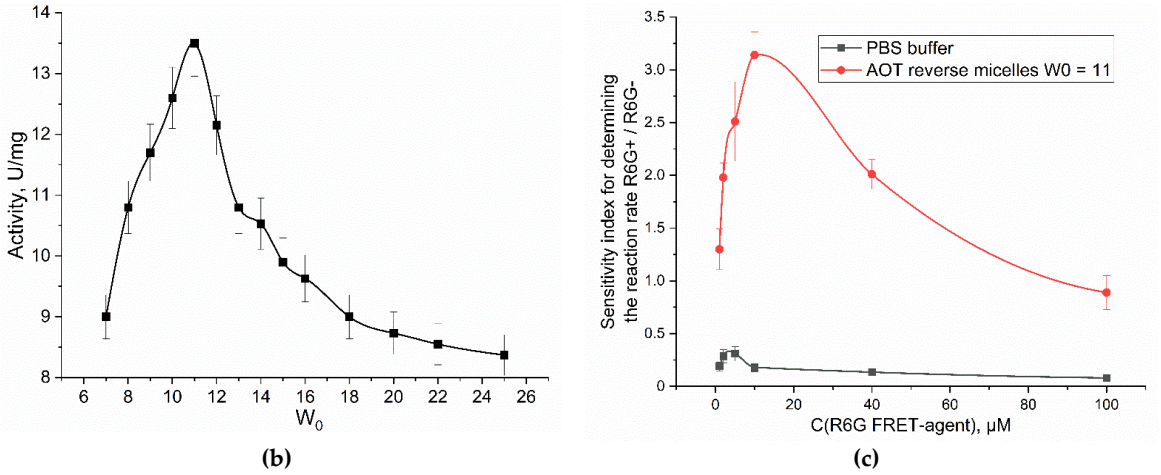

Figure 2. (a) The scheme of the catalytic hydrolysis reaction of MUTMAC using α-chymotrypsin. **(b)** The profile of the catalytic activity of chymotrypsin in the system of reversed AOT-octane micelles, depending on the hydration degree W_0. PBS (0.01M, pH 7.4) was used as aqueous phase. T = 37 °C. **(c)** Kinetic parameters of MUTMAC (0.2 mM) hydrolysis in the presence of chymotrypsin (6 μM) with FRET-marker R6G (variable concentration): sensitivity index for determining the rate of the MUTMAC hydrolysis reaction in the presence of FRET-agent R6G vs in the absence of R6G. For R6G+ system: λ_{exci} = 360 nm, λ_{emi} = 550 nm; for R6G– system: λ_{exci} = 360 nm, λ_{emi} = 450 nm. AOT/octane reverse micelles, W_0 = 11. T = 37 °C.

3.2.4. Acid Phosphatase Activity in Buffer Solution and in AOT-Octane Reverse Micelles

It is interesting to explore this phenomenon of the enhancement of FRET effect in the reversed micelles system for a membranotropic enzyme that functions in interaction with a micellar matrix compared with aqueous solution. Therefore, we chose acid phosphatase (membrane enzyme, hydrolase) as a model enzyme, which also (as α-chymotrypsin) releases the product MUmb during the enzymatic reaction. forming a donor-acceptor pair with R6G.

The dependence of the maximum rate of hydrolysis of 4-methylumbelliferyl phosphate (MUmb-phosphate) catalyzed by acid phosphatase in the system of reversed AOT cells on the degree of hydration of surfactants is a profile with two optima of enzyme activity at hydration degrees W_0 = 20 and 23-25 (Figure 5a). According to the principle of geometric correspondence, the optima of catalytic activity correspond to the coincidence of the size of the protein of the inner cavity of the micelle. Sedimentation analysis of the micellar system showed that at the hydration degree = 20, the enzyme functions as a monomer (48 kDa), and at W_0 = 24 as a dimer (98 kDa). At W_0 = 40, acid phosphatase can form tetramers and complexes with large organic molecules [31].

Figure 5 shows the profiles of phosphatase activity of acid phosphatase in the acetate buffer and in reversed micelles with hydration degrees W_0 = 20, 24 and 40. Detection was carried out by increasing the fluorescence of the initial reaction product (MUmb-phosphate -> MUmb) and by using the FRET- acceptor agent - R6G.

Again, in an aqueous solution, there is no special need for R6G: the reaction rate dI/dt = 240 (Figure 5bc), and only marginal energy is transmitted to R6G, that is, about 4% (Figure 5c). But in reversed micelles (W_0 = 40), the product signal (MUmb at 450 nm) is quenched, on the contrary R6G fluoresces more intensively. With a decrease in the hydration degree (micellar size), the fluorescence of MUmb decreases by 15-50% due to quenching, but FRET effect is still pronounced.

The observed rate of the enzymatic reaction tracked by R6G depends on the size of the reversed micelles. At W_0 = 20 or 24, about 10% of the fluorescence signal (velocity dI/dt) passes to R6G, and at W_0 = 40, about 13% of velocity is transferred to rhodamine. This is due to optimal size of the inner aqueous phase in the micelles in terms of FRET condition, including: places for enzyme, substrate and R6G. Thus, the observed dependence of the energy transfer efficiency to R6G on the product has a minimum at W_0 38-42. With high hydration degrees, we are gradually getting closer to the situation in an aqueous solution. At low degrees of hydration, the micelles have too small an internal cavity to

Preprints.org (www.preprints.org) | NOT PEER-REVIEWED | Posted: 31 May 2024 doi:10.20944/preprints202405.2096.v1

accommodate the optimal amount of substrate and FRET agent (R6G). The catalitic paramenter obtained using the new FRET approach are consistent with the literature data obtained by other methods [31,37].

It is worth noting that the FRET agent is used in a deficit (100-500 fold) to obtain comparable fluorescence values. It is possible to increase the amount of R6G, thereby significantly increasing the analytical signal and reducing the required amounts of substrate and enzyme. With an increase in the concentration of R6G by 5 and 20 times, the sensitivity of tracking product accumulation by the FRET marker rhodamine 6G increases by 2.5 and 6 times, respectively. In addition, the shift to the long-wavelength region increases the selectivity of the signal.

There is a significant disparity in the behavior of aqueous and membranotroic enzymes, as exemplified by chymotrypsin when compared with acid phosphatase, with regard to the use of FRET detection. The FRET agent enhances the sensitivity of detecting the reaction rate more effectively in the case of membrane enzymes due to the fact that, the enzyme is more densely surrounded by surfactant molecules and embedded within the membrane. Since enzymes containing carbohydrate or lipid groups have membrane-active properties, enzymes of the acid phosphatase are glycosylated. This results in their interaction with the micellar matrix and their high sensitivity to R6G.

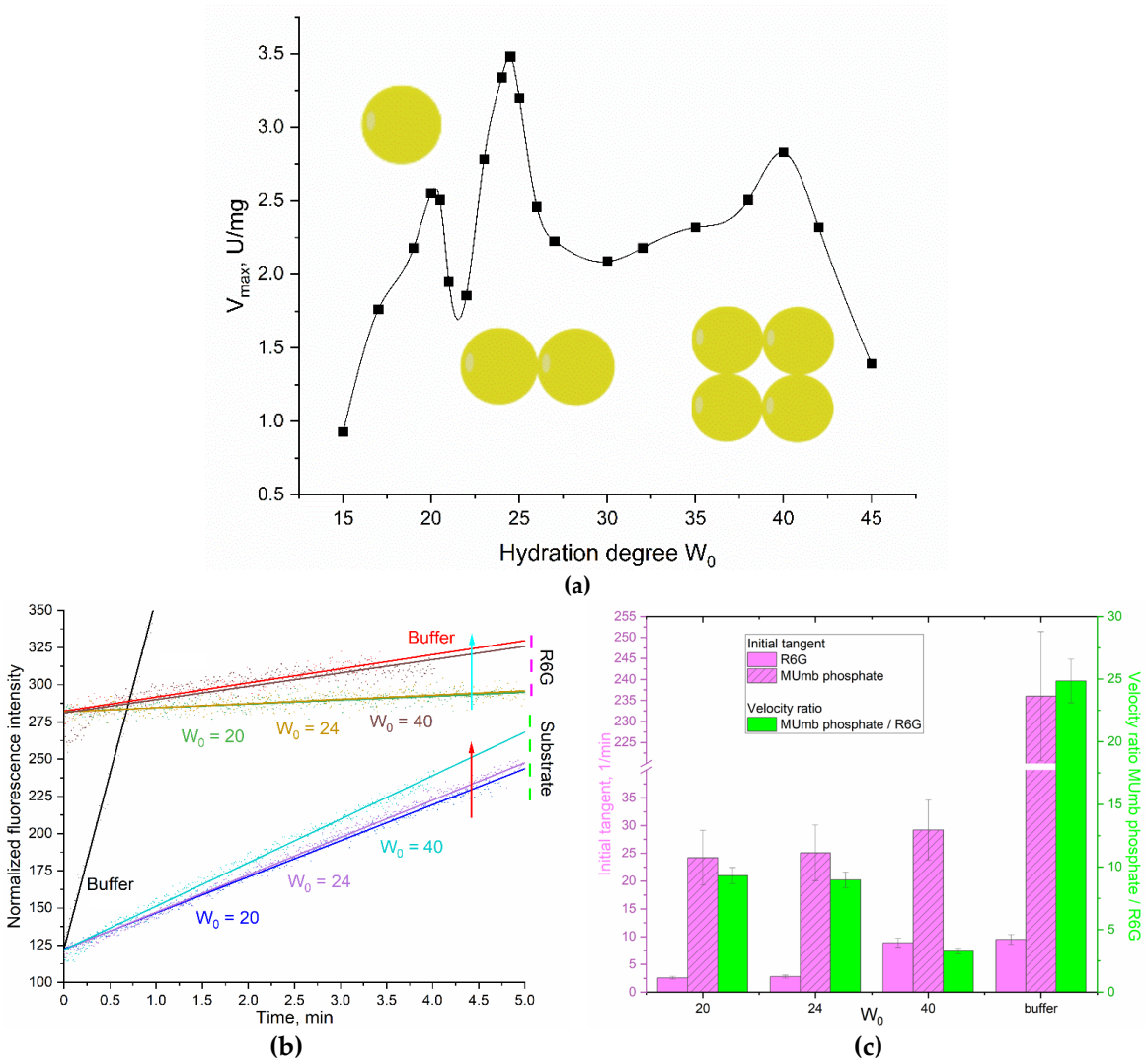

Figure 3. (a) The dependence of the catalytic activity (V_{max}) of acid phosphatase on the hydration degree of AOT (W_0) in the reverse micellar system. 0.1M AOT in octane was used as organic phase; KOAc/HOAc (0.01M, pH 4.9) was used as aqueous phase. T = 37 °C. **(b)** Phosphatase activity profiles curves of acid phosphatase (6 μM) in relation to MUmb-phosphate (0.8 mM) with FRET agent R6G-acceptor (2 μM). λ_{exci} = 360 nm, λ_{emi} = 450 (substrate – MUmb-phosphate and product – MUmb), 550

 doi:10.20944/preprints202405.2096.v1

(R6G) nm. AOT/octane reverse micelles. W_0 = 20, 24, 40. KOAc/HOAc (0.01M, pH 4.9) was used as aqueous phase. T = 37 °C. **(c)** Tangents of the initial linear sections of phosphatase profiles, the ratio of the initial "velocities" of the observed signals for the product and for the FRET agent R6G.

3.2.4. Catalytic Activity in a Two-Enzyme System: Alkaline Phosphatase and Asparaginase

Acid phosphatase functions at slightly acidic pH values (about 5-6), but it is important to study the FRET effect also in neutral – weakly alkaline pH (as in the bloodstream). To do this, we used alkaline phosphatase and asparaginase with pH optimum of about 8.0. Further FRET probes were applied to study the catalytic activity in a two-enzyme system.

Indeed, in the research practice in biochemistry there is often a need to study enzymatic reactions in two-enzyme systems: to increase the sensitivity of the signal, to study the mutual influence in the composition of enzymatic complexes, to study successive enzymatic reactions, to investigate biochemical chains in which the product of one enzyme is a substrate for another (bioconveyer), the effect of inhibition in cells biochemistry, etc. We suggest studying such reactions using FRET approach developed here. This may be both the parallel accumulation of one fluorophore donor or the accumulation of two consecutive fluorescence donors.

We chose L-asparaginase and alkaline phosphatase as model enzymes pair. For example, it would be useful to follow the asparaginase activity by R6G when analyzing the activity of asparaginase in the blood serum samples of patients in the treatment of leukemia. L-Asparaginase hydrolyzes the fluorescent substrate Asp-AMC to L-aspartate and AMC, and alkaline phosphatase hydrolyzes MUmb-phosphate to MUmb (Figure 4). The activity of the enzymes was studied in two enzyme systems with a hydration degree W_0 = 40, since both enzymes are active at such a W_0, and can be located in one micelle.

When using large micelles with a hydration degree of 40, the distance between the fluorophores of the FRETTED vapor approaches the value in an aqueous buffer solution (Figure 1e), which reduces the sensitivity.

Figure 6 shows the kinetic curves of the enzymatic activity of asparaginase, alkaline phosphatase and their mixed system. The initial linear sections are identified, from which the initial reaction rate can be determined (dI/dt), by initial products as well as by R6G fluorescence increase. Table 1 shows the parameter dI/dt of the initial linear region of kinetic curves.

In the case of L-asparaginase, approximately 20% of the (dI/dt) product passes to R6G. For alkaline phosphatase, this FRET characteristic is about 15%. In a two-enzyme system, the efficiency of FRET is in the range of 15-20%. Thus, we were able to monitor the enzymatic reactions of hydrolysis using R6G. In general, the obtained data are promising for practical applications in enzymological studies and visualization of processes in the cell using confocal microscopy to reduce autofluorescence.

Table 1. Initial rates of asparaginase and phosphatase kinetic profiles. AOT/octane reverse micellar system, W_0 = 40. The conditions are the same as indicated in the caption Figure 4.

Enzyme / Emission wavelength	Initial rate, 1/min (the observed values of tangents of linear sections of kinetic curves)			Specific activity, U/mg
	450 nm (AMC > MUmb)	465 nm (MUmb > AMC)	550 nm (R6G)	
L-Asparaginase	49±1	43±1	7.9±0.3	20±3
Alkaline phosphatase	57±4	48±4	8.4±0.5	2.1±0.6
Asparaginase + Alkaline phosphatase	82±6	105±7	16±1	17±4; 2.5±0.8

Preprints.org (www.preprints.org) | NOT PEER-REVIEWED | Posted: 31 May 2024 doi:10.20944/preprints202405.2096.v1

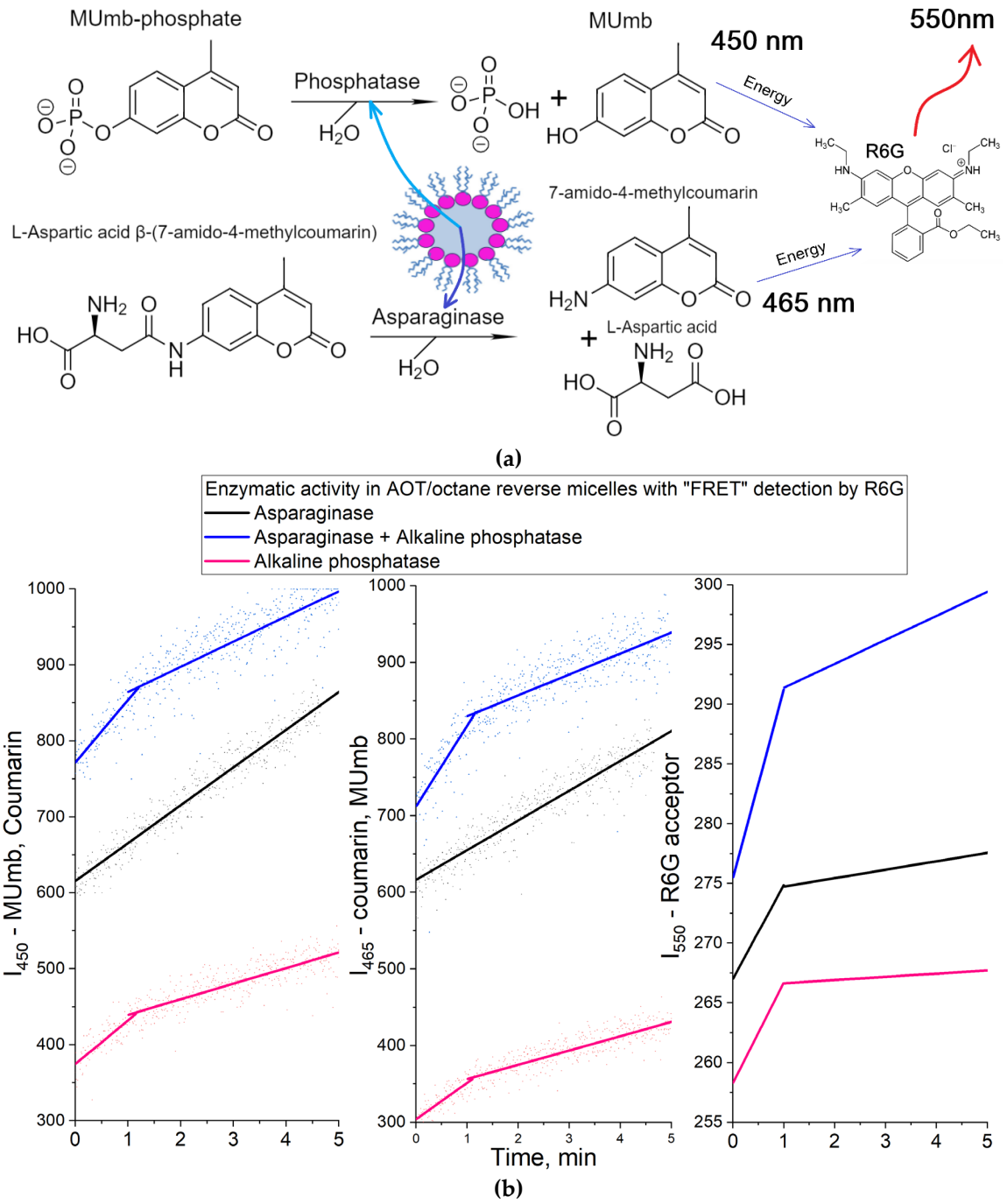

Figure 4. (a) Experiment design: Catalytic activity in a two-enzyme system: alkaline phosphatase and asparaginase. **(b)** Activity profiles curves of alkaline phosphatase (6 μM), asparaginase (1 μM) in relation to MUmb-phosphate (0.2 mM) and Asp-AMC (0.2 mM), correspondingly, with FRET agent R6G-acceptor (2 μM). λ_{exci} = 360 nm, λ_{emi} = 450 nm (product 1 – MUmb), 465 (product 2 –coumarin derivative), 550 nm (R6G – FRET agent). AOT/octane reverse micelles, W_0 = 40. PBS buffer (0.02M, pH 8.2). T = 37 °C.

Thus, using the examples of four enzymes, we have shown that it is possible to study catalysis using a FRET probe (R6G-acceptor), which makes it possible to significantly increase the anatomical signal and enhance its selectivity by shifting to the red region. In addition, the proposed methods are promising for use as visualizers of cellular structures and on-line reactions.

3.3. Visualization of Enzyme Activity in Living HEK293T Cells

 doi:10.20944/preprints202405.2096.v1

In medical practice, a variety of enzyme preparations are used, including asparaginase for the treatment of leukemia [38–44]. Therefore, targeted delivery of protein molecules to specific cells is a crucial task. The FRET technique allows us to study the intracellular activity of enzymes and determine the effectiveness of drug formulations.

Figure 5 shows confocal images HEK293T cells, which were pre-incubated with enzyme different times: in 1 hour, the enzyme practically did not accumulate in the cells, while in 6 hours, the accumulation of the enzyme was recorded. After that, the cells were placed in an agarose gel with a substrate MUTMAC, and during the enzymatic reaction, a fluorescent product MUmb accumulated. FRET is observed between the substrate or the product with FRET-agent R6G, which makes it possible to determine the accumulation of the latter due to enzymatic activity associated with cells.

It has been found that the FRET technique allows us to see firsthand the areas of depletion by the substrate (donor) and enrichment by the product, exactly at the sites of cell localization – in the case of intracellular activity. And we observe an even fluorescent background in the case of asparaginase, which did not internalize into cancer cells. This demonstrates the usefulness of the FRET method for determining enzymatic activity and studying the effectiveness of drugs.

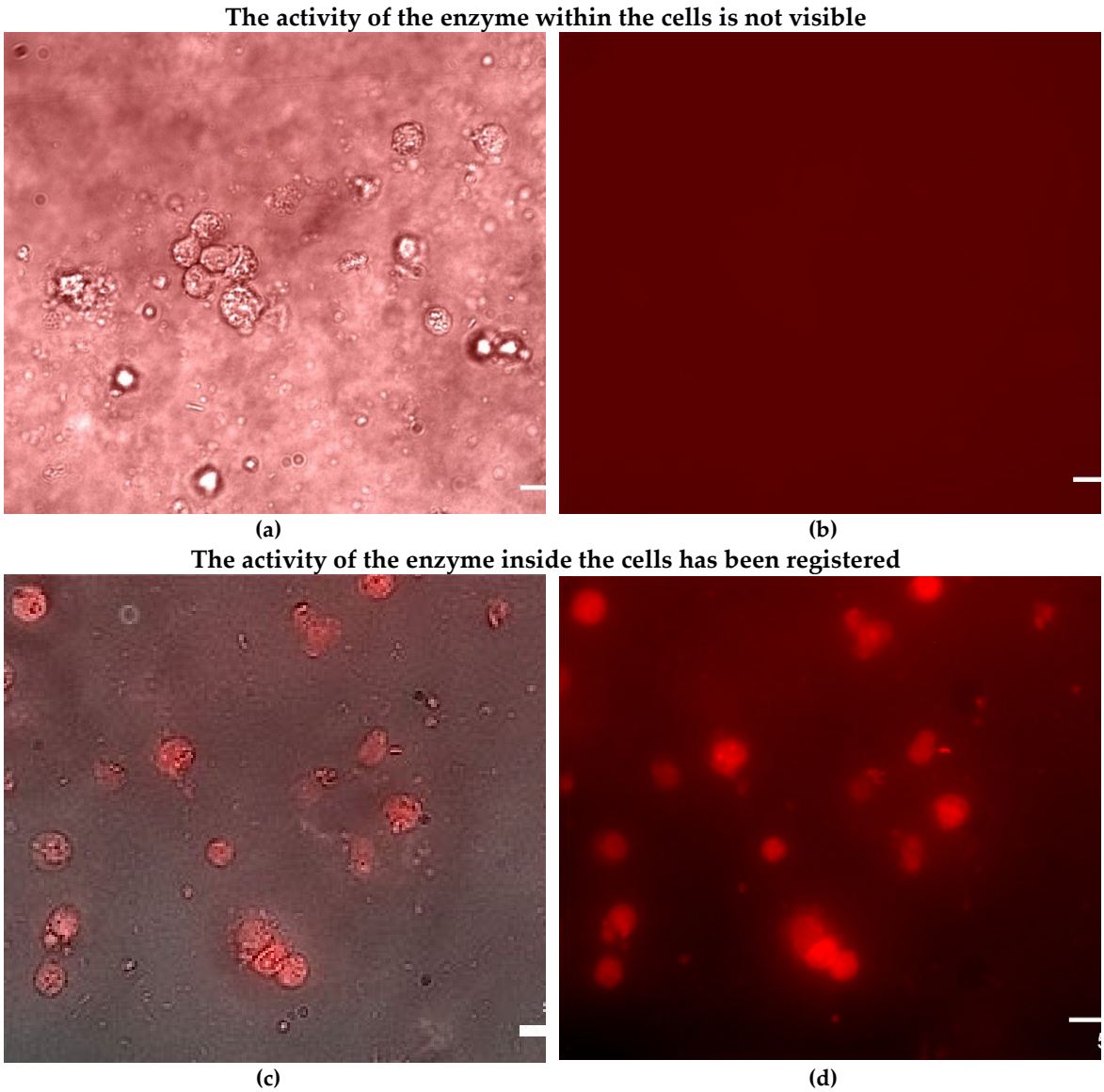

Figure 5. Confocal fluorescence images of HEK293T cells (with absorbed L-asparaginases) in agarose gel containing 1 mg/mL MUTMAC and 1 μM FRET-agent R6G. T = 37 °C. C_0(enzyme) = 0.5 mg/mL. λ_{exci} = 515 nm, λ_{emi} = 540-600 nm. The scale segment is 50 μm. (a), (b) - images of cells after 1 hour

 doi:10.20944/preprints202405.2096.v1

incubation with the enzyme: merged and R6G fluorescent channel; (c), (d) - images of cells after 4 hours incubation with the enzyme: merged and R6G fluorescent channel.

4. Conclusions

In this paper, we propose the use of the fluorescence resonance energy transfer (FRET) probe technique, specifically the Rhodamine 6G (R6G), 4-methylumbelliferone (MUmb), and 7-amino-4-methylcoumarin (AMC) derivative, as a tool for studying enzymatic activity. The proposed method allows for the study of enzymatic activity without relying on product detection, and instead using the FRET signal as a marker. This approach has the potential to increase the efficiency and specificity of the assay, as well as the possibility of translating the technique to living cells. Four model enzymes were investigated: acidic and alkaline phosphatase, asparaginase, and chymotrypsin, in aqueous media and reverse AOT-octane micelle systems. In these systems, it was challenging to directly determine the parameters of enzymatic catalysis from the AMC or MUmb product signal. However, by using the R6G FRET marker, we were able to improve the sensitivity of the technique up to 20-fold. We found that the FRET efficiency varied between 5 and 20%, depending on the system composition and enzyme type. The intracellular activity of asparaginase and the non-specific activity of the enzyme observed using FRET technique can be seen as two opposing aspects of the function of medical enzymes – what is important for determining the specificity of the formulation. The data obtained is promising in terms of studying enzymatic activity in reverse micelle systems as well as living cells.

Author Contributions: Conceptualization, E.V.K. and I.D.Z.; methodology, I.D.Z., A.A.E., E.V.K.; formal analysis, I.D.Z., A.A.E.; investigation, I.D.Z., A.A.E., and E.V.K.; data curation, I.D.Z., A.A.E.,; writing—original draft preparation, I.D.Z.; writing—review and editing, E.V.K.; project supervision, E.V.K.; funding acquisition, E.V.K. All authors have read and agreed to the published version of the manuscript.

Funding: This research was funded by the Russian Science Foundation, grant number 24-25-00104.

Data Availability Statement: The data presented in this study are available in the main text.

Institutional Review Board Statement: HEK293T cell line was obtained from Lomonosov Moscow State University Depository of Live Systems Collection (Moscow, Russia).

Informed Consent Statement: Not applicable.

Acknowledgments: The work was performed using the equipment (FTIR microscope MICRAN-3, Jasco J-815 CD Spectrometer, AFM microscope NTEGRA II) – of the program for the development of Moscow State University.

Conflicts of Interest: The authors declare no conflicts of interest.

Abbreviations

AMC – 7-amino-4-methylcoumarin; AOT – bis(2-ethylhexyl) sulfosuccinate or diisooctyl sulfosuccinate; FRET—Förster resonance energy transfer; MUmb – 4-methylumbelliferone or methylumbelliferyl; MUTMAC – 4-methylumbelliferyl p-trimethylammoniocinnamate chloride; R6G – rhodamine 6G; W_0 – degree of hydration of reversed micelles.

References

1. Algar, W.R.; Hildebrandt, N.; Vogel, S.S.; Medintz, I.L. FRET as a biomolecular research tool — understanding its potential while avoiding pitfalls. *Nat. Methods* **2019**, *16*, 815–829, doi:10.1038/s41592-019-0530-8.
2. Chen, T.; He, B.; Tao, J.; He, Y.; Deng, H.; Wang, X.; Zheng, Y. Application of Förster Resonance Energy Transfer (FRET) technique to elucidate intracellular and In Vivo biofate of nanomedicines. *Adv. Drug Deliv. Rev.* 2019, *143*, 177–205.
3. Zhou, X.; Su, F.; Lu, H.; Senechal-Willis, P.; Tian, Y.; Johnson, R.H.; Meldrum, D.R. An FRET-based ratiometric chemosensor for in vitro cellular fluorescence analyses of pH. *Biomaterials* **2012**, *33*, 171–180, doi:10.1016/j.biomaterials.2011.09.053.

4. Lone, M.S.; Afzal, S.; Nazir, N.; Dutta, R.; Dar, A.A. Excimer based FRET between non-FRET pair flourophores aided by the aromatic moiety of anionic surfactants: An experimental observation. *J. Mol. Liq.* **2019**, *277*, 84–92, doi:10.1016/j.molliq.2018.11.118.
5. Bhat, P.A.; Chat, O.A.; Dar, A.A. Exploiting Co-solubilization of Warfarin, Curcumin, and Rhodamine B for Modulation of Energy Transfer: A Micelle FRET On/Off Switch. *ChemPhysChem* **2016**, 2360–2372, doi:10.1002/cphc.201600274.
6. Guo, C.; Yuan, H.; Yu, Y.; Gao, Z.; Zhang, Y.; Yin, T.; He, H.; Gou, J.; Tang, X. FRET-based analysis on the structural stability of polymeric micelles: Another key attribute beyond PEG coverage and particle size affecting the blood clearance. *J. Control. Release* **2023**, *360*, 734–746, doi:10.1016/j.jconrel.2023.07.026.
7. Zlotnikov, I.D.; Savchenko, I. V; Kudryashova, E. V Specific FRET Probes Sensitive to Chitosan-Based Polymeric Micelles Formation, Drug-Loading, and Fine Structural Features. *Polymers (Basel).* **2024**, *16*, 739, doi:10.3390/polym16060739.
8. Zhang, H.; Li, H.; Cao, Z.; Du, J.; Yan, L.; Wang, J. Investigation of the in vivo integrity of polymeric micelles via large Stokes shift fluorophore-based FRET. *J. Control. Release* **2020**, *324*, 47–54, doi:10.1016/j.jconrel.2020.04.046.
9. Shrestha, D.; Jenei, A.; Nagy, P.; Vereb, G.; Szöllősi, J. *Understanding FRET as a research tool for cellular studies*; 2015; T. 16; ISBN 3652532201.
10. Jares-Erijman, E.A.; Jovin, T.M. FRET imaging. *Nat. Biotechnol.* **2003**, *21*, 1387–1395, doi:10.1038/nbt896.
11. Wu, L.; Huang, C.; Emery, B.P.; Sedgwick, A.C.; Bull, S.D.; He, X.-P.; Tian, H.; Yoon, J.; Sessler, J.L.; James, T.D. Förster resonance energy transfer (FRET)-based small-molecule sensors and imaging agents. *Chem. Soc. Rev.* **2020**, *49*, 5110–5139, doi:10.1039/C9CS00318E.
12. Hoffmann, S.; Gorzelanny, C.; Moerschbacher, B.; Goycoolea, F.M. Physicochemical characterization of FRET-labelled chitosan nanocapsules and model degradation studies. *Nanomaterials* **2018**, *8*, doi:10.3390/nano8100846.
13. Watrob, H.M.; Pan, C.P.; Barkley, M.D. Two-step FRET as a structural tool. *J. Am. Chem. Soc.* **2003**, *125*, 7336–7343, doi:10.1021/ja034564p.
14. Panniello, A.; Trapani, M.; Cordaro, M.; Dibenedetto, C.N.; Tommasi, R.; Ingrosso, C.; Fanizza, E.; Grisorio, R.; Collini, E.; Agostiano, A.; и др. High-Efficiency FRET Processes in BODIPY-Functionalized Quantum Dot Architectures. *Chem. - A Eur. J.* **2021**, *27*, 2371–2380, doi:10.1002/chem.202003574.
15. Saxena, S.; Pradeep, A.; Jayakannan, M. Enzyme-Responsive Theranostic FRET Probe Based on l -Aspartic Amphiphilic Polyester Nanoassemblies for Intracellular Bioimaging in Cancer Cells. *ACS Appl. Bio Mater.* **2019**, *2*, 5245–5262, doi:10.1021/acsabm.9b00450.
16. Yang, G.; Li, C.; Fischer, M.; Cairo, C.W.; Feng, Y.; Withers, S.G. A FRET Probe for Cell-Based Imaging of Ganglioside-Processing Enzyme Activity and High-Throughput Screening. *Angew. Chemie* **2015**, *127*, 5479–5483, doi:10.1002/ange.201411747.
17. Paquin, F.; Rivnay, J.; Salleo, A.; Stingelin, N.; Silva, C. Multi-phase semicrystalline microstructures drive exciton dissociation in neat plastic semiconductors. *J. Mater. Chem. C* **2015**, *3*, 10715–10722, doi:10.1039/b000000x.
18. Krasteva, G.; Pfeil, U.; Drab, M.; Kummer, W.; König, P. Caveolin-1 and -2 in airway epithelium: Expression and in situ association as detected by FRET-CLSM. *Respir. Res.* **2006**, *7*, 1–13, doi:10.1186/1465-9921-7-108.
19. Yang, Y.; Liu, H.; Han, M.; Sun, B.; Li, J. Multilayer Microcapsules for FRET Analysis and Two-Photon-Activated Photodynamic Therapy. *Angew. Chemie Int. Ed.* **2016**, *55*, 13538–13543, doi:10.1002/anie.201605905.
20. König, P.; Krasteva, G.; Tag, C.; König, I.R.; Arens, C.; Kummer, W. FRET-CLSM and double-labeling indirect immunofluorescence to detect close association of proteins in tissue sections. *Lab. Investig.* **2006**, *86*, 853–864, doi:10.1038/labinvest.3700443.
21. Meng, F.; Sachs, F. Orientation-based FRET sensor for real-time imaging of cellular forces. *J. Cell Sci.* **2012**, *125*, 743–750, doi:10.1242/jcs.093104.
22. Kikuchi, K.; Takakusa, H.; Nagano, T. Recent advances in the design of small molecule-based FRET sensors for cell biology. *TrAC - Trends Anal. Chem.* **2004**, *23*, 407–415, doi:10.1016/S0165-9936(04)00608-9.
23. Lindenburg, L.; Merkx, M. Engineering genetically encoded FRET sensors. *Sensors (Switzerland)* **2014**, *14*, 11691–11713, doi:10.3390/s140711691.
24. Kaminski Schierle, G.S.; Bertoncini, C.W.; Chan, F.T.S.; van der Goot, A.T.; Schwedler, S.; Skepper, J.; Schlachter, S.; van Ham, T.; Esposito, A.; Kumita, J.R.; и др. A FRET Sensor for Non-Invasive Imaging of Amyloid Formation in Vivo. *ChemPhysChem* **2011**, *12*, 673–680, doi:10.1002/cphc.201000996.
25. Sahu, K.; Ghosh, S.; Mondal, S.K.; Ghosh, B.C.; Sen, P.; Roy, D.; Bhattacharyya, K. Ultrafast fluorescence resonance energy transfer in a micelle. *J. Chem. Phys.* **2006**, *125*, 1–9, doi:10.1063/1.2218847.
26. Ilhami, F.B.; Bayle, E.A.; Cheng, C.C. Complementary nucleobase interactions drive co-assembly of drugs and nanocarriers for selective cancer chemotherapy. *Pharmaceutics* **2021**, *13*, 1–18, doi:10.3390/pharmaceutics13111929.

27. Ngan, V.T.T.; Chiou, P.Y.; Ilhami, F.B.; Bayle, E.A.; Shieh, Y.T.; Chuang, W.T.; Chen, J.K.; Lai, J.Y.; Cheng, C.C. A CO2-Responsive Imidazole-Functionalized Fluorescent Material Mediates Cancer Chemotherapy. *Pharmaceutics* **2023**, *15*, doi:10.3390/pharmaceutics15020354.
28. Zehentbauer, F.M.; Moretto, C.; Stephen, R.; Thevar, T.; Gilchrist, J.R.; Pokrajac, D.; Richard, K.L.; Kiefer, J. Fluorescence spectroscopy of Rhodamine 6G: Concentration and solvent effects. *Spectrochim. Acta - Part A Mol. Biomol. Spectrosc.* **2014**, *121*, 147–151, doi:10.1016/j.saa.2013.10.062.
29. Zlotnikov, I.D.; Malashkeevich, S.M.; Belogurova, N.G.; Kudryashova, E. V. Thermoreversible Gels Based on Chitosan Copolymers as "Intelligent" Drug Delivery System with Prolonged Action for Intramuscular Injection. *Pharmaceutics* **2023**, *15*, doi:10.3390/pharmaceutics15051478.
30. Kudryashova, E. V.; Leferink, N.G.H.; Slot, I.G.M.; Van Berkel, W.J.H. Galactonolactone oxidoreductase from Trypanosoma cruzi employs a FAD cofactor for the synthesis of vitamin C. *Biochim. Biophys. Acta - Proteins Proteomics* **2011**, *1814*, 545–552, doi:10.1016/j.bbapap.2011.03.001.
31. Kudryashova, E. V.; Bronza, V.L.; Vinogradov, A.A.; Kamyshny, A.; Magdassi, S.; Levashov, A. V. Regulation of acid phosphatase in reverse micellar system by lipids additives: Structural aspects. *J. Colloid Interface Sci.* **2011**, *353*, 490–497, doi:10.1016/j.jcis.2010.09.072.
32. Creagh, A.L.; Prausnitz, J.M.; Blanch, H.W. Structural and catalytic properties of enzymes in reverse micelles. *Enzyme Microb. Technol.* **1993**, *15*, 383–392, doi:10.1016/0141-0229(93)90124-K.
33. Maitra, A.; Ghosh, P.K.; De, T.K.; Sahoo, S.K. Process for the preparation of highly monodispersed polymeric hydrophilic nanoparticles. **1997**, 5.
34. Jia, H.; Zhu, G.; Wang, P. Catalytic Behaviors of Enzymes Attached to Nanoparticles: The Effect of Particle Mobility. *Biotechnol. Bioeng.* **2003**, *84*, 406–414, doi:10.1002/bit.10781.
35. Blocher, M.; Walde, P.; Dunn, I.J. Modeling of enzymatic reactions in vesicles: The case of ?-chymotrypsin. *Biotechnol. Bioeng.* **1999**, *62*, 36–43, doi:10.1002/(SICI)1097-0290(19990105)62:1<36::AID-BIT5>3.0.CO;2-U.
36. Kudryashova, E. V.; Artemova, T.M.; Vinogradov, A.A.; Gladilin, A.K.; Mozhaev, V. V.; Levashov, A. V. Stabilization and activation of α-chymotrypsin in water-organic solvent systems by complex formation with oligoamines. *Protein Eng.* **2003**, *16*, 303–309, doi:10.1093/proeng/gzg039.
37. Luchter-Wasylewska, E.; Iciek, M. Positive cooperativity in substrate binding of human prostatic acid phosphatase entrapped in AOT-isooctane-water reverse micelles. *J. Colloid Interface Sci.* **2004**, *273*, 632–637, doi:10.1016/j.jcis.2004.01.075.
38. Batool, T.; Makky, E.A.; Jalal, M.; Yusoff, M.M. A Comprehensive Review on l-Asparaginase and Its Applications. *Appl. Biochem. Biotechnol.* **2016**, *178*, 900–923, doi:10.1007/s12010-015-1917-3.
39. Fonseca, M.H.G.; Fiúza, T. da S.; Morais, S.B. de; Souza, T. de A.C.B. de; Trevizani, R. Circumventing the side effects of L-asparaginase. *Biomed. Pharmacother.* **2021**, *139*, doi:10.1016/j.biopha.2021.111616.
40. Burke, M.J.; Zalewska-Szewczyk, B. Hypersensitivity reactions to asparaginase therapy in acute lymphoblastic leukemia: Immunology and clinical consequences. *Futur. Oncol.* **2022**, *18*, 1285–1299, doi:10.2217/fon-2021-1288.
41. Egler, R.A.; Ahuja, S.P.; Matloub, Y. L-asparaginase in the treatment of patients with acute lymphoblastic leukemia. *J. Pharmacol. Pharmacother.* **2016**, *7*, 62–71, doi:10.4103/0976-500X.184769.
42. Krasotkina, J.; Borisova, A.A.; Gervaziev, Y. V; Sokolov, N.N. One-step purification and kinetic properties of the recombinant L -asparaginase from Erwinia carotovora. *Biotech. Appl. Biochem.* **2004**, *39*, 215–221.
43. Douer, D.; Gökbuget, N.; Stock, W.; Boissel, N. Optimizing use of L-asparaginase–based treatment of adults with acute lymphoblastic leukemia. *Blood Rev.* **2022**, *53*, doi:10.1016/j.blre.2021.100908.
44. Mohideen, A.K.S. Molecular docking study of L-Asparaginase i from Vibrio campbellii in the treatment of acute lymphoblastic leukemia (ALL). *Eurobiotech J.* **2020**, *4*, 8–16, doi:10.2478/ebtj-2020-0002.